

Growth and Characterization of the Laterally Enlarged Single Crystal Diamond Grown by Microwave Plasma Chemical Vapor Deposition

Ze-Yang Ren(任泽阳), Jin-Feng Zhang(张金凤)**, Jin-Cheng Zhang(张进成)**, Sheng-Rui Xu(许晟瑞),
Chun-Fu Zhang(张春福), Kai Su(苏凯), Yao Li(李姚), Yue Hao(郝跃)

State Key Discipline Laboratory of Wide Band-Gap Semiconductor Technology, School of Microelectronics,
Xidian University, Xi'an 710071

(Received 7 March 2018)

Laterally enlarged single crystal diamond is grown on (001) diamond substrates by microwave plasma chemical vapor deposition. Based on the largest side-to-side width of the seed of 7.5 mm, we achieve the as-grown epilayer with the width of about 10 mm between the same two sides. The luminescence difference between the broadened part of the single crystal diamond and the vertically epitaxial part is investigated by characterizing the vertical cross section of the sample, and the possible growth mechanism is suggested. Vertical epitaxy on the top (001) surface and lateral growth on the side surfaces occur simultaneously, and thus the growth fronts along the two directions adjoin and form a coalescence zone extending from the edge of the substrate towards the edge of the expanded single crystal diamond top surface. The luminescence intensity of the nitrogen-vacancy center is relatively high in the coalescence zone and a laterally grown part right below, which are attributed mainly to the higher growth rate. However, stress change and crystal quality change are negligible near the coalescence zone.

PACS: 81.05.ug, 81.15.Gh, 68.55.Ln

DOI: 10.1088/0256-307X/35/7/078101

Diamond has been considered as the ultimate semiconductor material due to its state-of-the-art properties, such as wide band gap, high breakdown voltage, and high carrier mobility.^[1,2] However, the lack of large substrates hindered the development of single crystal diamond (SCD) severely. Recent years, several methods are developed to obtain large area single crystal diamond plate.^[3–6] Among these methods, the so-called mosaic wafers have been realized in the largest area over 2 inch.^[7,8] However, this method still needs the separated large high quality single diamond plates. As we know, during SCD epitaxy, a poly crystal diamond (PCD) rim usually appears around the SCD, which induces the shrinkage of the SCD top surface. To effectively eliminate the PCD rims, the pocket substrate holder was developed and optimized by several groups,^[9,10] and then even the SCD top surface expanding was realized.^[5] In addition, keeping a constant temperature of the SCD surface during growth is also very important to achieve the effective top surface expanding. Recently, the SCD epitaxy with the top surface expanding to almost twice the one of the substrate was reported.^[5] However, whether the broadened part of the SCD shows the same crystal quality and impurity density with the vertically epitaxial part has never been investigated to the best of our knowledge. Obviously, the property uniformity of the SCD is of great interest for either semiconductor applications or gem usage.

In this Letter, we investigate luminescence properties of a vertical cross section of laterally enlarged SCD grown by microwave plasma chemical vapor deposition (MPCVD), and suggest the possible growth mechanism.

The type Ib high-pressure high-temperature (HPHT) (100) diamond substrates we used include the square plates with {100} sides or {110} sides, and an octagonal plate with four {110} sides and four {100} sides. All substrates were polished to achieve the rms surface roughness below 1 nm, and were cleaned in boiling H₂SO₄/HNO₃ (1:1) mixture at 250°C for one hour to remove the non-diamond phase. Then the substrates were etched by the hydrogen plasma with 2% oxygen added for 30 min to remove polishing-induced mechanical damage. Before growth, each substrate was brazed on a molybdenum holder using 25-μm-thick gold foil to achieve the stable thermal exchange between the diamond sample and the chiller under the holder. The purity of the hydrogen and the methane used for growth is 6N and 5N5, respectively. In the process of the growth, the pressure, temperature, and microwave power are 320 mbar, 915°C, and 3.9 kW, respectively. The total gas flow rate of 200 sccm and the methane concentration of 6% were used. During the growth, we lower the sample at a rate of 20 μm/h to keep a constant temperature of the sample surface.

After growth, the SCD growth rate of about 19 μm/h was evaluated by a digital micrometer. The morphology of the sample was observed using differential interference-contrast microscopy (DICM). The crystalline property was characterized at room temperature (RT) using scanning electron microscopy (SEM) with cathodoluminescence (CL) unit attached, and Raman and photoluminescence (PL) spectra (both with a 514 nm laser). The acceleration voltage for CL measurements was 10 kV.

The 0.6-mm-thick SCD epilayer grown on the 3 mm × 3 mm seed with {100} sides shows a largest

**Corresponding author. Email: jfzhang@xidian.edu.cn; jchzhang@xidian.edu.cn
© 2018 Chinese Physical Society and IOP Publishing Ltd

width of 4.5 mm and no PCD rims appear (Figs. 1(a) and 1(c)). However, the shrinkage of the top surface compared with the measured largest size of the sample occurs distinctly with four corners truncated. This is similar to the result reported in Refs. [11,12] and can be explained by the development of the $\{113\}$ faces at the corner.^[13] The $\{113\}$ faces have the slowest growth rate in the SCD growth, and are prone to twinning and defect nucleation at the corners inducing stress and cracks. The epilayer after substrate removal and polishing shows highly defective corners with cracks (not shown here).

The 1.2-mm-thick epilayer grown on the $3\text{ mm} \times 3\text{ mm}$ seed with $\{110\}$ sides (Figs. 1(b) and 1(d)) is surrounded by PCD rims and the largest sample width is 5.5 mm (with both PCD rims and the SCD epilayer accounted for). The top surface also shrinks compared with the measured largest size of the sample, and this could be attributed to the easy appearance of the $\{113\}$ faces at the $\{110\}$ sides.

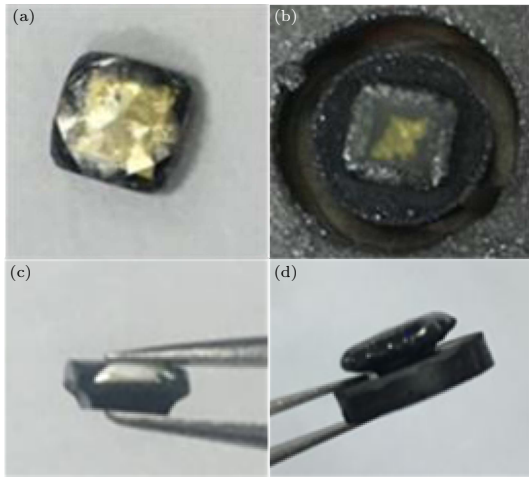


Fig. 1. Top view of as-grown SCD epilayer on $\{001\}$ HPHT with (a) $\{100\}$ and (b) $\{110\}$ sides, and side view of as-grown SCD epilayer on HPHT $\{001\}$ diamond seed with (c) $\{100\}$ and (d) $\{110\}$ sides.

The sample grown on the octagonal seed with alternating $\{110\}$ and $\{100\}$ sides also shows the enlargement of the epilayer (Figs. 2(a) and 2(b)). Based on the largest side-to-side width of the seed of 7.5 mm between the two $\{110\}$ sides, we have achieved the as-grown epilayer with the width of above 10 mm between the same two sides at a thickness of 1.4 mm. Meanwhile, the top surface shows only a very slight area decrease at $\{110\}$ sides compared with the largest transverse section of the epilayer. Though PCD appears at the $\{110\}$ sides, all the $\{100\}$ side surfaces are clean with very good transparency. The effective enlargement of the top surface, or the effective maintenance of the largest transverse section appeared in the growth, is ascribed to the change of shape of the seed and the growth mechanisms. The octagonal seed has no corners towards the $\langle 110 \rangle$ direction, thus the corner problem for $\{100\}$ sides (Figs. 2(a) and 2(b)) is

eliminated. As for the growth at $\{110\}$ sides, the coexistence of the $\{100\}$ sides may restrain the formation of the $\{113\}$ facet in the growth, thus the center-edge morphology predominates.^[9] The epilayer after substrate removal and polishing shows a largest side-to-side width of 9.97 mm (as shown in Fig. 2(c)). The full width at half maximum of the (004) rocking curve is measured to be 37.91 arcsec (Fig. 2(d)), which is comparable with the result of the electronic grade single crystal diamond (34.98 arcsec) commercially obtained from Element Six Ltd. The DICM images of the sample surface at $\{100\}$ and $\{110\}$ sides (Figs. 3(a) and 3(b)) show the typical step-bunching morphology of single crystal extending to exactly the $\{100\}$ side and the clear transition from internal SCD to twins and PCD at the $\{110\}$ side.

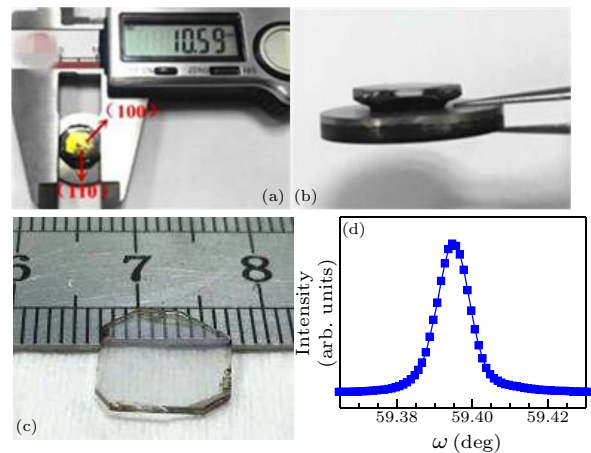


Fig. 2. Top view (a) and side view (b) of the as-grown SCD on an octagonal seed with alternating $\{110\}$ and $\{100\}$ sides, (c) epilayer after substrate removal and polishing, and (d) (004) XRD rocking curve of the CVD grown SCD.

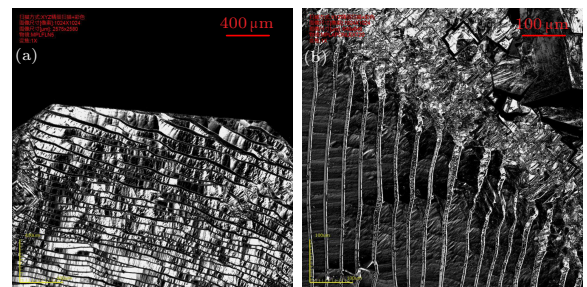


Fig. 3. DICM images of the sample top surface bounded by (a) $\{100\}$ side and by (b) $\{110\}$ side.

To investigate the property of the laterally enlarged SCD, after initial lateral enlargement growth of SCD on the $3 \times 3\text{ mm}^2$ square substrate with $\{100\}$ sides, we exposed the vertical cross section of the sample (inset in Fig. 4(a)) by laser cutting and mechanical polishing, and characterized it using SEM and CL (Fig. 4(a)). The lateral enlargement of the SCD is distinct and no PCDs appear at the sides of the enlarged SCD. In addition, the lateral growth rate is larger than the vertical one, which is similar to the result reported

in Ref. [5]. This may be ascribed to higher concentrations of carbon species in the gases and the higher temperature at side surfaces as suggested by the simulation results of Ref. [14].

One can see clearly in the CL image (Fig. 4(a)) the lateral and vertical interfaces between the substrate and the CVD grown diamond as dark lines, and also the (113) facet at the sample corner as a dark region. Meanwhile, a wedge-like bright region extends from the edge of the substrate towards the (113) facet, but is separated from the facet by a dark quadrilateral region. Just below the wedge and quadrilateral regions there is a long illuminant band. To investigate the luminescence property of these regions, we measured the CL spectra at different locations (points 1–3 in Fig. 2(a)). Point 1 locates in the substrate. Point 3 is right above the substrate, and point 2 locates in the illuminant band below the wedge region. The CL spectrum of point 2 (Fig. 4(b)) is similar to the result of CVD SCD reported in Ref. [15]. The spectrum of point 2 shows an intense broad illuminant peak ranging from 550 nm to 700 nm generally ascribed to the nitrogen-vacancy (NV) center. [15] In addition, there is a weak peak near 504 nm well known as H3-center, originating from nitrogen atom inclusions and dislocations. As for the result of point 1, a peak of band-A appears at 430 nm except for the peak of H3-center, which indicates the presence of incoherent grain boundaries and dislocations inside the substrate and much more nitrogen atom inclusions. These results hint that the brightness in the CL image (Fig. 2(a)) is mainly induced by the NV centers.

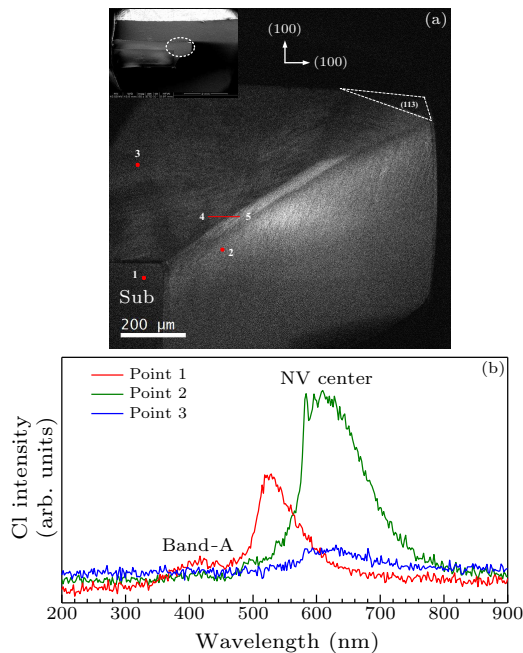


Fig. 4. (a) CL image with SEM image (inset) of the cross section of the SCD grown on the $3 \times 3 \text{ mm}^2$ substrate, and (b) CL spectra of points 1–3.

Therefore, the luminescence distribution in Fig. 4(a) indicates the difference in impurity incorpo-

ration and the possible growth mechanism of our laterally enlarged SCD. The wedge region with the highest luminescence intensity, or the highest density of NV centers, is in fact the fastest grown part in the sample. As vertical epitaxy on the top (001) surface and faster lateral growth on the {001} side surfaces occur simultaneously, the growth fronts along the two directions adjoin at the edge of the substrate. The vertical atom-layer deposition forms a protruding ‘template’ for the lateral atom-layer deposition, and vice versa, and the dynamic growth forms the wedge-like coalescence zone (C-zone) extending towards the edge of the top surface. Meanwhile, the higher temperature and density of reactive species at edges of the top surface [14] lead to the most active atom incorporation in the C-zone. The dark quadrilateral region separating the C-zone and the (113) facet is ascribed to the extending (113) growth domain originating from the apex of the diamond substrate. The much-reduced luminescence in the domain needs further investigation. The long illuminant band shows more NV centers concentrated just below the C-zone and the (113) domain than in the other laterally grown part, and this may be due to the relatively large growth rate and the nitrogen incorporation efficiency influenced by the gas flow direction from above to the side of the epilayer.

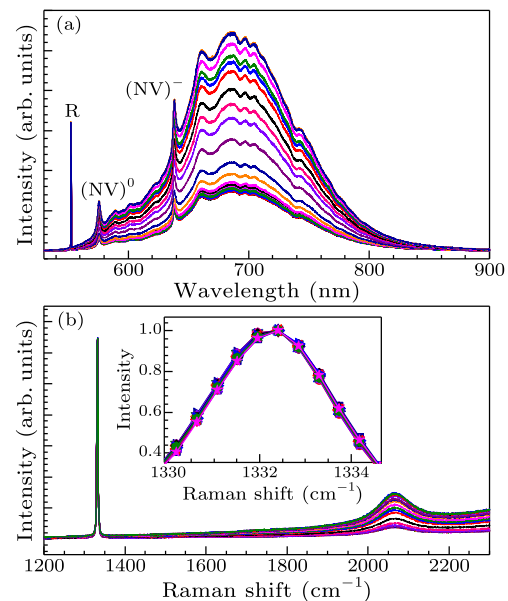


Fig. 5. Line scanning results of (a) PL and (b) Raman spectra from point 4 to point 5 in Fig. 4(a).

To further investigate the properties of the C-zone, we measured the line scanning results of PL and Raman near the C-zone. The typical PL peaks (Fig. 5(a)) at 575 nm and 638 nm, related to (NV)⁰ and (NV)⁻, respectively, are observed. [16] Meanwhile, there is an intense broad band ranging from 600 to 800 nm, which was considered as the associated phonon replicas of NV-related zero phonon lines. [17] The intensity of the broad band increases significantly and becomes stronger than the NV-related peaks and Raman peak

R (552 nm)^[18] when measured at the C-zone. This indicates that more NV centers are in the C-zone, and it agrees with the CL results. The strong Raman scattering peaks for the diamond phase (Fig. 5(b)) at about 1332 cm^{-1} can be observed and no peaks for the non-diamond phase appear, which indicates the high quality of the SCD. The position and the width of the diamond-related Raman peak show almost no change along the scanning line, which indicates that the changes of both stress and crystal quality near the C-zone are negligible. In addition, the peak at about 2100 cm^{-1} related to nitrogen can be observed, and the changing of this peak agrees with the PL and CL results.

In conclusion, we have grown SCDs on high-pressure high-temperature substrates with different side surfaces and achieved the growth of laterally enlarged SCD. The analysis of CL images and local CL spectra of the vertical cross section of the laterally enlarged SCD shows that the local brightness in the CL image is mainly induced by the NV centers, and the luminescence distribution is mainly attributed to the different growth-rate-related impurity incorporations in the sample. The zone formed by the coalescence of the vertical and lateral growth front extends from the edge of the substrate towards the edge of the SCD top surface, and shows the highest growth rate and thus the strongest NV-center-related CL, PL, and Raman peaks. However, Raman results show that the changes of both stress and crystal quality near the zone are negligible.

References

- [1] Zhang H, Li S S, Su T C, Hu M H, Li G H, Ma H G and Jia X P 2016 *Chin. Phys. B* **25** 098101
- [2] Isberg J, Hammersberg J, Johansson E, Wikstrom T, Twitchen D J, Whitehead A J, Coe S E and Scarsbrook G A 2002 *Science* **297** 1670
- [3] Mokuno Y, Chayahara A, Yamada H and Tsubouchi N 2009 *Diamond Relat. Mater.* **18** 1258
- [4] Mokuno Y, Chayahara A, Yamada H and Tsubouchi N 2010 *Diamond Relat. Mater.* **19** 128
- [5] Charris A, Nad S and Asmussen J 2017 *Diamond Relat. Mater.* **76** 58
- [6] Nad S, Gu Y and Asmussen J 2015 *Diamond Relat. Mater.* **60** 26
- [7] Yamada H, Chayahara A, Mokuno Y, Tsubouchi N and Shikata S 2013 *Diamond Relat. Mater.* **33** 27
- [8] Yamada H, Chayahara A, Mokuno Y, Kato Y and Shikata S 2014 *Appl. Phys. Lett.* **104** 102110
- [9] Nad S and Asmussen J 2016 *Diamond Relat. Mater.* **66** 36
- [10] Wu G, Chen M H and Liao J 2016 *Diamond Relat. Mater.* **65** 144
- [11] Tallaire A, Achard J, Silva F, Brinza O and Gicquel A 2013 *CR Phys.* **14** 169
- [12] Silva F, Achard J, Bonnin X, Brinza O, Michau A, Secroun A, De Corte K, Felton S, Newton M and Gicquel A 2008 *Diamond Relat. Mater.* **17** 1067
- [13] Silva F, Achard J, Bonnin X, Michau A, Tallaire A, Brinza O and Gicquel A 2006 *Phys. Status Solidi A* **203** 3049
- [14] Yamada H, Chayahara A, Mokuno Y, Horino Y and Shikata S 2006 *Diamond Relat. Mater.* **15** 1738
- [15] Chayahara A, Mokuno Y, Horino Y, Takasu Y, Kato H, Yoshikawa H and Fujimori N 2004 *Diamond Relat. Mater.* **13** 1954
- [16] Li H D, Zou G T, Wang Q L, Cheng S H, Li B, Lue J N, Lue X Y and Jin Z S 2008 *Chin. Phys. Lett.* **25** 1803
- [17] Achard J, Silva F, Brinza O, Tallaire A and Gicquel A 2007 *Diamond Relat. Mater.* **16** 685
- [18] Tallaire A, Collins A T, Charles D, Achard J, Sussmann R, Gicquel A, Newton M E, Edmonds M and Cruddace R J 2006 *Diamond Relat. Mater.* **15** 1700